

# POLYMER-MODIFIED CEMENT ASPHALT MORTAR AS INTERLAYER IN THE NON-BALLASTED TRACK OF HIGH-SPEED TRAIN

Aditya Wahyu Erlangga<sup>1</sup>, Latif Budi Suparma<sup>\*2</sup>, Suprpto Siswosukarto<sup>3</sup>

<sup>1,2,3</sup> Department of Civil and Environmental Engineering, Universitas Gadjah Mada, Indonesia

<sup>\*</sup>Corresponding Author, Received: 14 June 2023, Revised: 06 Dec. 2023, Accepted: 14 Jan. 2024

**ABSTRACT:** Non-ballasted track consists of a concrete slab bonded firmly to the concrete base by a cement asphalt mortar (CAM) as an interlayer for damping. In practice, interface bonding failure occurs on CAM. Styrene-butadiene rubber (SBR) polymer is proposed as a modifying material to increase the interface bonding strength of CAM. The problem of polymer modification in CAM is probably related to poor compatibility and workability. This study aims to investigate the effect of the SBR polymer pH value on the compatibility and workability in CAM. Compatibility is determined by separation rate. Zeta potential value describes polymer-modified asphalt emulsion (PMAE) activity. Workability is determined by funnel fluidity time and slump flow time. Results showed that increasing the SBR polymer pH value decreased the zeta potential of PMAE. Decreasing zeta potential to be value-neutral results in destabilized asphalt droplets, demulsified, separated water, and asphalt coalescence. Finally, the asphalt coalescence is covered by polymer and forms a binding film on cement. It is affecting the compatibility between PMAE and cement hydration. It results in a low separation rate. Compatibility is achieved by SBR polymer pH 10.0 doses ranging from 1% to 6%. SBR polymer dosage of 1% to 3% led to a deceleration in funnel fluidity time and slump flow time associated with elevated demulsification. Their 4% to 6% dose accelerates funnel fluidity time and slump flow time associated with delaying demulsification. Acceptance of compatibility and workability in CAM is proposed using SBR polymer pH 10.0 dosage of 4% to 6%.

*Keywords:* Non-ballasted track, cement asphalt mortar, polymer-modified cement asphalt mortar, polymer-modified asphalt emulsion, SBR polymer, polymer pH, workability, compatibility.

## 1. INTRODUCTION

As a popular transportation, the train has a new genre of high-speed train [1,2]. High-speed trains have been developed in Japan, China, and Indonesia [3]. There are two high-speed railway tracks: a ballasted track and a non-ballasted track [4].

Non-ballasted track of a high-speed train consists of a precast concrete slab bonded to a continuous concrete base firmly by a cement asphalt mortar (CAM) layer [5], as shown in Fig. 1. The primary purpose of the CAM interlayer is to provide bonding, elasticity, and damping and decrease dynamic movement experienced by the track system [6-8].

The CAM material comprises asphalt emulsion, cement, sand, and other additives [7]. Cationic asphalt emulsion is used as CAM material because its properties ensure strength in the early stage [9]. It has a lower retardation effect on the hydration process than anionic asphalt emulsion [10]. All these ingredients are mixed and then grouted into the space between the precast concrete slab and the concrete base. The grouting process's success relies on CAM's workability characteristics and how well it will form a composite system [11].

According to the Chinese Railway Specification, 2008 CN 18598016A, the CAM properties are shown in Table 1.

In practice, the CAM layer and the concrete slab bear the external load on the non-ballasted track system. The flexural strength of composite slabs is primarily determined by the interface bonding strength between the CAM and the concrete slab [7]. The problem of CAM application arises with interface bonding failure caused by external loads and the cycle of gradual temperature changes over a certain period [13].

Table 1 Specification of CAM (Chinese Railway Specification, 2008) [12].

Properties	Properties Index
Workability:	$D_5 \geq 280$ mm, time $D_{280\text{ mm}} \leq 16$ s
Slump flow time	$D_{30} \geq 280$ mm, time $D_{280\text{ mm}} \leq 22$ s
Funnel fluidity time	80 s to 120 s
Separation rate	$\leq 3\%$

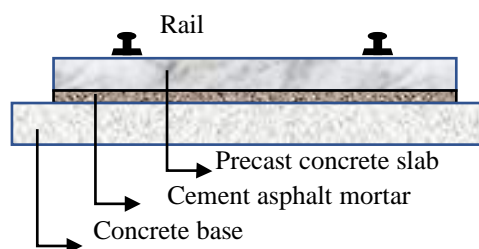


Fig. 1 Nonballasted track with CAM interlayer.

Polymers with excellent adhesive properties are proposed as modifying materials to increase the interface bonding strength of CAM [7,14]. Styrene butadiene rubber (SBR) polymer as a modifying material in CAM can improve mechanical properties [15]. In the process, the SBR polymer is used in polymer-modified asphalt emulsion (PMAE) as the material in CAM [15]. The problem of polymer modification in CAM is related to poor compatibility and workability [9] [16-19].

Compatibility between asphalt and cement must be verified to ensure the success of polymer modification [18,19]. It is crucial for achieving homogeneity and workability in the CAM [9,19]. Therefore, intensive investigations should continue to be carried out on compatibility and workability. Ho T studied the performance of CAM modified with polymer and proposed that compatibility occurs when the asphalt can bond to the cement hydration product without separation. It is affected by the asphalt emulsion activity [19]. Wang F reported that compatibility occurs when the  $\text{Ca}(\text{OH})_2$  concentration of cement hydration neutralizes the acid in the asphalt emulsion [11]. Fang L studied the interaction between cement and asphalt emulsion and revealed that compatibility is affected by the adsorption of cement mineral components to emulsified asphalt [9]. Liang P studied the compatibility of SBR-modified asphalt and reported that compatibility is related to the stability of PMAE [16]. Fazhou W [20] studied the chemical stability of asphalt emulsion, and Cui D [21] studied the effect of pH on the cationic bitumen emulsifier properties. They reported that the polymer pH affects asphalt emulsifiers' stability and surface activity [20,21]. The activity of asphalt emulsion droplets can be assessed by determining the charges of zeta potential [22].

On the other hand, the polymer component contributes to the demulsification of asphalt emulsion, which can significantly decrease workability [9,19]. When the demulsification reaction occurs before the final mixing is completed, it can significantly increase the viscosity of the mixed materials, thereby decreasing workability [9,19].

Studies on the effect of polymer pH value are still limited to the surface activity of asphalt emulsions. However, the effect of polymer pH value on the compatibility between asphalt emulsion and cement in CAM and workability in CAM as an interlayer in the non-ballasted track still needs to be determined. Therefore, this remains to be seen and requires further study.

This study aims to systematically investigate the effect of the SBR polymer pH value on CAM's compatibility and workability as an interlayer in the non-ballasted track. In the initial stages, the effect of the SBR polymer pH value on the activity of asphalt emulsion is studied. The zeta potential value is used to assess the effect of the SBR polymer pH value on the charge of PMAE droplets, directly impacting their activity. The obtained value elucidates PMAE and

cement hydration compatibility in CAM mixtures. The index of the separation rate is used to assess compatibility. The effect of SBR polymer dosage on the workability characteristics of CAM is studied in a subsequent stage. Indexes such as funnel fluidity time and slump flow time determined these characteristics.

## 2. RESEARCH SIGNIFICANCE

This research is expected to set a firmer theoretical foundation of polymer-modified CAM characteristics as an interlayer in the non-ballasted track, where special attention is given to the effect of the pH value of SBR polymer and their dosage on the compatibility and workability of CAM and to bring novel insight into the optimal design of the non-ballasted track structure.

## 3. EXPERIMENTAL STUDY

### 3.1. Material

This study used the slow-setting cationic asphalt emulsion following the ASTM D2397, which has a value saybolt furol viscosity (24°C) of 31 s, storage stability of 24 hours, and 0.71%, distillation residue of 59.43%. Ordinary Portland cement (OPC) of type I, following ASTM C 150, is used in the study. River sand with gradation II, following ASTM C 33, is utilized, with a grain modulus of 3.0. SBR polymer is developed to enhance the compatibility and workability properties of CAM.

It was set to have pHs of 7.1, 9.1, and 10.0, representing neutral, weak, and strong bases, respectively. The properties of SBR polymer are outlined in Table 2.

Table 2 Properties of SBR polymer

Polymer	Solid content (%)	Density ( $\text{gr}/\text{cm}^3$ )	Viscosity (cPs)	pH
SBR 1	± 40%	1.01	< 100	7.1
SBR 2	± 40%	1.02	-	9.1
SBR 3	38,19%	1.02	1000 – 2500	10.0

### 3.2. Mixing Method of CAM

The dry mix technique is employed in this study. This method is recommended, associated with the proper and homogeneous dispersion of the polymer with the bitumen [23]. The mixing process is conducted with Hobart N50, following the ASTM C 305-99, 2008 standard method.

The process is initiated by preparing dry components using a mixer set at 60 rpm for 60 seconds. Separately, the liquid components are mixed at 60 rpm for 60 seconds. Subsequently, the liquid and dry components are mixed with a mixer speed of 60 rpm for 60 seconds. The speed is then decreased to 124 rpm for 30 seconds, then back to 60 rpm for another 60 seconds to ensure the consistency of the CAM mixture. The

expansive agent is added in the final stage, stirring at 60 rpm for 90 seconds. The fresh mixture is ready for the test.

### 3.3. Composition of CAM

The asphalt emulsion to cement ratio (AE/C) is 0.2, while that of sand to cement (S/C) is 1.0. The water-cement factor (W/C) is fixed at 0.34. The variations of SBR polymer pH of 7.1, 9.1, and 10.0 represented a neutral, weak, and strong base, respectively [21], as shown in Table 3. The variations in SBR polymer doses are shown in Table 4.

### 3.4. Test Method

#### 3.4.1. Separation rate test of CAM

The separation rate method involved three specimens of cube CAM with dimensions of 50 mm. Each specimen is cut equally in the middle, resulting in two equal parts. The density of each part is then determined using the ASTM C642-97. The following equation is applied to calculate the separation rate of hardened CAM [24]:

$$S = \frac{L-U}{L+U} \times 100\% \quad (1)$$

Where S (%) = separation rate of hardened CAM, L (kg/m<sup>3</sup>) = density of the lower part CAM, and U (kg/m<sup>3</sup>) = density of the upper part CAM.

#### 3.4.2. The workability of CAM

The workability of CAM is determined by funnel fluidity time and slump flow time according to Chinese Railway Specifications (2008). The funnel fluidity time test method follows ASTM C 939-10. A slump flow time method is conducted following ASTM C1611M using standard ASTM C230M-03 mold. There are two sets of tests to evaluate for acceptance of slump flow time. In the first, after mixing CAM for 5 minutes (D5), it is measured at the time of the flow at a diameter of 280 mm (D5-t280 mm). Finally, after mixing it for another 30 minutes (D30), it is measured at the time of the flow at a diameter of 280 mm (D5-t280 mm).

#### 3.4.3. Zeta potential test

A zeta potential analyzer is utilized to assess the charge of asphalt emulsion droplets, directly impacting their stability. 100 ml of asphalt emulsion is used, and the SBR polymer pH is adjusted to 5% by the weight of the asphalt emulsion.

#### 3.4.4. Microstructure of CAM

A scanning electron microscope (SEM) is used to investigate the microstructure of CAM.

#### 3.4.5. pH characteristic of the asphalt emulsion

pH meter is utilized to measure the PMAE pH.

## 4. RESULTS AND DISCUSSIONS

### 4.1 Effect of pH Value of SBR Polymer on Compatibility in CAM.

Figure 2 presents the effect of SBR polymer pH on CAM's separation rate. The results of non-polymer samples, SBR polymer pH 7.1 and pH 9.1 resulted in very high separation rates of 16.32%, 15.72%, and 15.07%, while in Table 1, the acceptance requirement < 3%. It is indicated that separation occurs between PMAE and hydrated cement. The hydrated cement components settle downward, while the asphalt particles precipitate settle upward, as shown in Fig. 3.a, b, and c. It shows the incompatibility between PMAE and hydrated cement. PMAE failed to bond with hydrated cement, resembling concrete mortar without asphalt, as shown in Fig. 8. a.

Table 3 Composition of CAM with a variation of SBR polymer pH

Code	P/C	SBR Polymer pH
P 1	0%	-
P 2	4%	7.1
P 3	4%	9.1
P 4	4%	10.0

Description: P = SBR polymer C = cement

Table 4 Composition of CAM with variation doses of SBR polymer

Code	A1	A2	A3	A4	A5	A6	A7	A8
P/C	0%	1%	2%	3%	4%	5%	6%	9%

Description: P = SBR polymer; C = cement

Figure 4 presents the effect of the SBR polymer pH on PMAE's pH value. In non-polymer samples, SBR polymer pH 7.1 and SBR polymer pH 9.1 resulted in PMAE pH values of 3.7, 4.5, and 5.9. This value indicates under acidic conditions and strong cationic [20,21]. According to Wang F, asphalt emulsion at acidic pH conditions, without being neutralized, cannot bind to cement hydration products [11].

Compatibility between asphalt emulsion and cement can be affected by the stability of asphalt emulsion [25]. The properties of asphalt emulsion are affected by pH value [23]. The pH value of the polymer affected the surface activity of the asphalt emulsifiers [21].

Figure 5 presents the effect of the pH value of SBR polymer on the zeta potentials of PMAE. In non-polymer samples, SBR polymer pH 7.1 and SBR polymer pH 9.1 result in PMAE zeta potential of +37.1 mV, +33.2 mV, and +30.1 mV, respectively. A value of > +30 mV indicates strong cationic [26]. As a result, the dispersed droplets have a stable dispersion state, as shown in Fig. 6. a, b, and c. A zeta potential greater than +30.0 mV indicates strong cationic and has colloid stability characteristics [22,26].

During the cement hydration process, various ions, such as  $\text{Ca}^{2+}$ ,  $\text{SO}_4^{2-}$ ,  $\text{K}^+$ ,  $\text{Na}^+$ , and  $\text{OH}^-$ , are released at different concentrations [20]. Among them,  $\text{Ca}^{2+}$  is the primary constituent that acts as a counter ion and is used to evaluate the compatibility between asphalt emulsion and cement [20].

On the non-polymer samples, SBR polymer pH 7.1 and pH 9.1 result in PMAE having a positive charge and a stable coalescence upon contact with cement, which carries a positive charge of  $\text{Ca}^{2+}$  [20]. As a result, electrification cohesion occurs [20]. It leads to separating PMAE and hydrated cement, as presented in Fig. 3. a, b, and c. PMAE failed to form a bond with the hydrated cement, indicating incompatibility between PMAE and cement hydration in CAM.

Figure 4 shows the pH value of PMAE adjusted to 7.3, indicating neutral [27]. This condition results in a low separation rate of 0.83%. A value  $<3\%$  meets CAM acceptance requirements, as in Fig. 2 for sample P4.

On sample P4, an asphalt emulsion is added with SBR polymer pH 10.0, resulting in the zeta potential decrease from +37 mV to +10.9 mV, which indicates approximate neutrality [26]. As a result, the droplets lose stability, demulsify, and flocculate rapidly, as shown in Fig. 6. d. This phenomenon is supported by Fazhou W stated that increasing the pH of emulsified asphalt leads to a decrease in positive charge and rapid flocculation of droplets. Upon contact with cement carrying a positive charge of  $\text{Ca}^{2+}$ , electrification adhesion takes place [20]. PMAE effectively binds to the cement hydration. It shows PMAE and cement hydration compatibility in CAM, as presented in Fig. 3. d. According to Wang F [11], asphalt emulsion at neutral pH conditions can bind to cement hydration products.

The compatibility phase between PMAE and cement involved several essential steps. Starting from: 1) The cationic asphalt emulsion droplets exist in stable colloid conditions, as shown in Fig. 6.a. 2) When SBR polymer pH 10.0 is added to the asphalt emulsion, the droplets rapidly lose stability, are demulsified, and rapidly flocculated, as shown in Fig. 6.d, which separates water from the emulsion. In this case, the lost stability of droplets occurs because the SBR polymer pH 10.0 becomes strongly anionic, causing dispersion electrification upon contact with cationic asphalt emulsion. During initial mixing, the strongly anionic polymer attracted the positive charge field of the cationic asphalt emulsion. This attraction allows the molecules to bond with the outer layer of the asphalt emulsion layer. Lu C [25] explained that negatively charged droplets of SBR polymer come into contact with their positively charged counterpart. 3) The SBR polymer ( $\text{CH}^-$ ), which acts as the outer layer of asphalt emulsion ( $\text{CH}^+$ ), remains negatively charged. When in contact with cement ( $\text{Ca}^{2+}$ ), electrification adhesion occurs, enabling the SBR polymer to bind with this ion. Plank [28] stated that  $\text{Ca}^{2+}$  ions are consumed by hydration and adsorbed on particles with a negative charge. 4) When water is absorbed by cement,

hydration takes place. The double layer of SBR polymer and asphalt coalescence is bonded with cement hydration. 5) During the hardening phase of the CAM structure, the asphalt coalescence layer covered by polymer forms a binding film on cement ( $\text{Ca}^{2+}$ ). The compatibility between PMAE and cement results in a CAM structure without separation, as shown in Fig. 8.b.

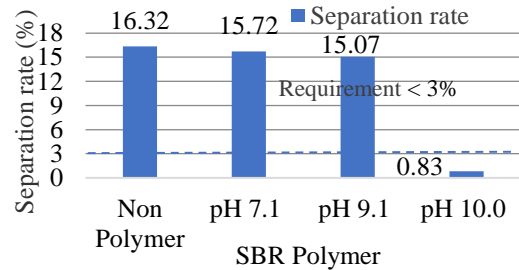


Fig. 2 Separation rate of the CAM

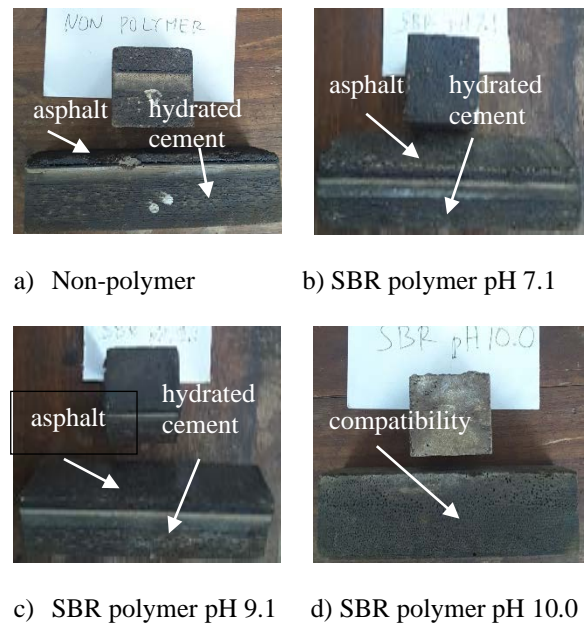


Fig. 3 Separation between PMAE and hydrated cement in CAM

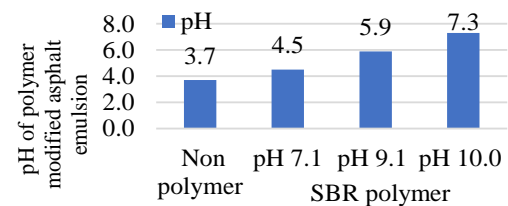


Fig. 4 The effect of the pH value of SBR polymer on pH PMAE

The schematic illustration in Fig. 7 provides an overview of the compatibility phase between PMAE and cement.



According to Wang F [11], the interaction phase between cement and asphalt occurred when the concentration of  $\text{Ca}(\text{OH})_2$  induced by cement hydration neutralized the acid in asphalt emulsion, gradually forming hydration products. Cement granules and hydration products will absorb asphalt droplets. In the dispersion state, this interaction led to the breaking of cement hydration and asphalt emulsion [11]. However, according to Fazhou [20], the concentration of  $\text{Ca}^{2+}$  had only a slight effect on the stability on the stability of cationic asphalt emulsion. Based on the recent results, the compatibility between polymer-modified cationic asphalt emulsion and cement is affected by the colloid stability characteristics of asphalt emulsion, which in turn is affected by the pH value of the polymer.

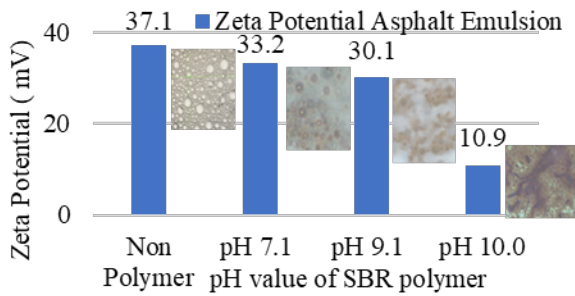


Fig. 5 Zeta potential of PMAE

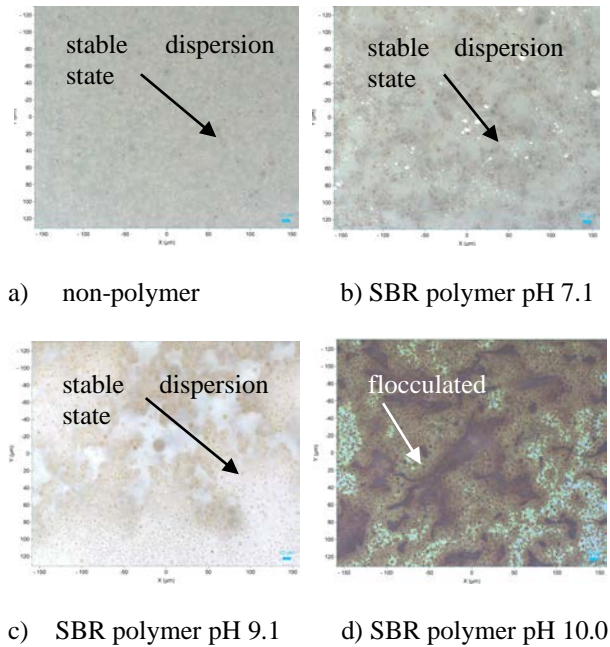


Fig. 6 Stability colloid of PMAE \*(x20 of scale)

Furthermore, increasing the pH value of the polymer resulted in a decrease in the zeta potential of asphalt emulsion. As the zeta potential decreased from a strongly cationic value of +37.1 mV to +10.9 mV, indicating approximate neutrality, the asphalt droplets rapidly lost stability, demulsified, and fluctuated the interaction between SBR-polymer-pH 10.0 and asphalt

results in the demulsification of asphalt droplets and water separation. The asphalt layer covered by SBR polymer forms a binding film on the hydrated cement at the hardening phase.

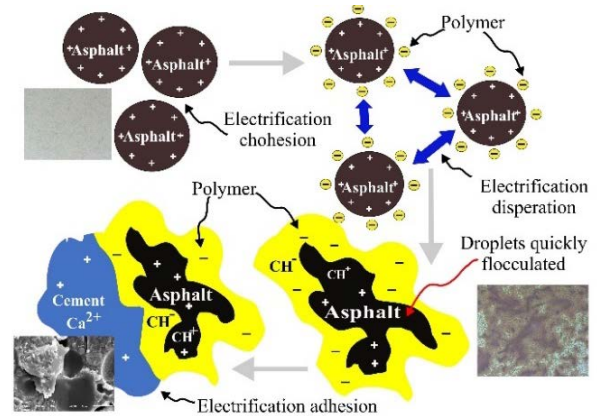
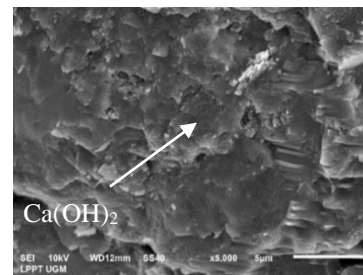
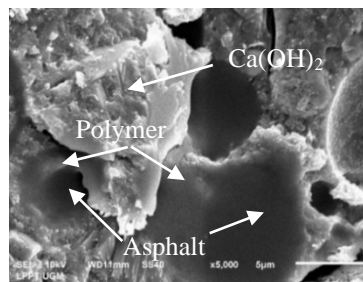


Fig. 7 The schematic illustration compatibility between PMAE and cement in CAM



a) Incompatibility asphalt emulsion and cement



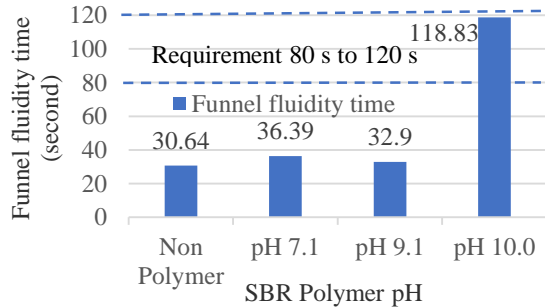
b) Compatibility asphalt emulsion and cement

Fig. 8 Microstructure of CAM

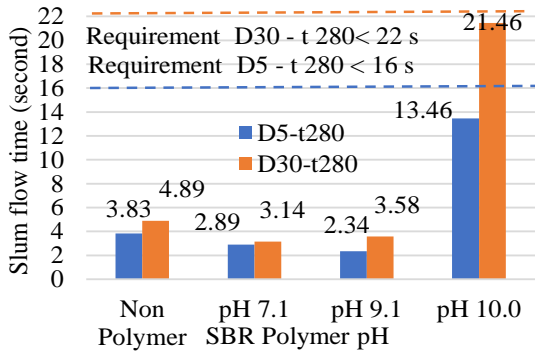
#### 4.2 Effect of the pH value of SBR polymer on the workability of CAM

The workability characteristics of CAM are determined by funnel fluidity time and slump flow time. Figure 9 presents the effect of the SBR polymer pH on the funnel fluidity time and slump flow time. In the non-polymer samples, SBR polymer pH 7.1 and 9.1 resulted in funnel fluidity times of 30.64 s, 36.39 s, and 32.9 s, respectively. It is much faster than the sample SBR polymer pH 10.0, which gave a time of 118.83 s.

Their slump flow times D5-t280 are 3.83 s, 2.89 s, and 2.34 s, respectively, and D 30-t280 are 4.89 s, 3.14 s, and 3.58 s, respectively. It is much faster than sample P4, which results in 13.46 s for D5-t280 and 21.46 s for D 30-t280.



a) Funnel fluidity time

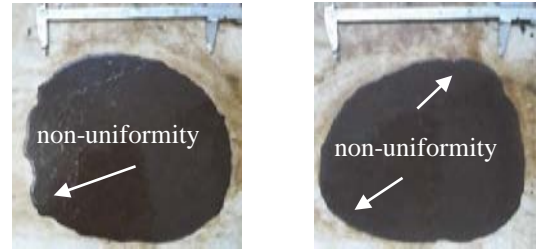


b) Slump flow time

Fig. 9 The effect of the SBR polymer pH on funnel fluidity time and slump flow time

In the non-polymer samples, SBR polymer pH 7.1 and pH 9.1, resulted in the PMAE failing to bind on cement hydration, and separation occurred between PMAE and cement. It leads to a low yield stress in the fresh CAM, accelerating funnel fluidity time and slump flow time, as shown in Fig. 9. Lower yield stress results in fresh CAM, suggesting increased self-flowing ability [29]. Consequently, this also causes non-uniformity in the slump flow of fresh CAM, as shown in Fig. 10. Non-uniformity slump flow is a flow that is different at different locations along the flow path [30].

In the SBR polymer pH 10.0 sample, the polymer-modified asphalt could bind to the cement hydration without separation. It leads to a deceleration in funnel fluidity time and slump flow time, as shown in Fig. 9. The higher yield stress of fresh paste indicates the decreased self-flowing ability of fresh CAM [29]. Consequently, this also causes uniformity in the slump flow of fresh CAM, as shown in Fig. 9. d. Uniformity slump flow is a flow that is uniform at different locations along the flow path [30].



a) Non-polymer

b) SBR Polymer pH 7.1



c) SBR polymer pH 9.1



d) SBR polymer pH 10.0

Fig. 10 The effect of the pH value of SBR polymer on the uniformity flow of CAM

### 4.3 Effect of SBR polymer dosage on the workability of CAM

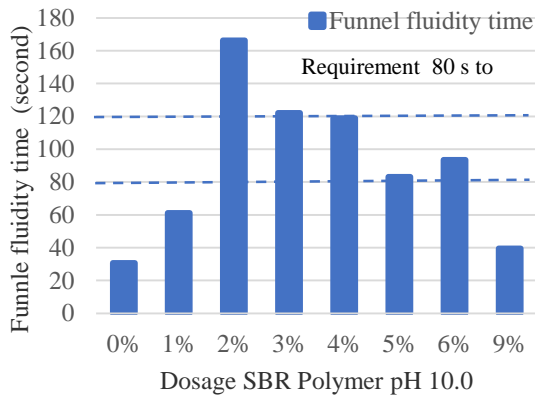
Figure 11 presents the effect of SBR polymer pH 10.0 dosage on CAM's funnel fluidity time and slump flow time. The non-polymer CAM showed a funnel fluidity time of 30,64 s and slump flow time of 3.83 s for D5-280 and 4.89 s for D30-t280, much faster than the specification CAM Table 1. In the case of non-polymer CAM, the asphalt droplets fail to bond with the cement. It leads to a low yield stress in the fresh CAM, accelerating funnel fluidity time and slump flow time. The yield stress is lower in fresh CAM, suggesting increased self-flowing ability [29]. Consequently, this also causes non-uniformity in the slump flow of fresh CAM, as shown in Fig. 12. a.

SBR polymer dosage of 1% to 3% in CAM led to a decrease in funnel fluidity time from 61.14 s to 122.2 s, and their slump flow time D5-280 has slowed from 13.58 s to 17.52s and D30-t280 from 14.02 s to 26.52 s. It is suspected that the polymers contributed to the increase in the asphalt emulsion demulsification process and increased the bonding to the cement hydration. The demulsification of asphalt emulsion is associated with increases in the yield stress and viscoelasticity of fresh CAM, which is indicated by a deceleration in funnel fluidity time and slump flow time.

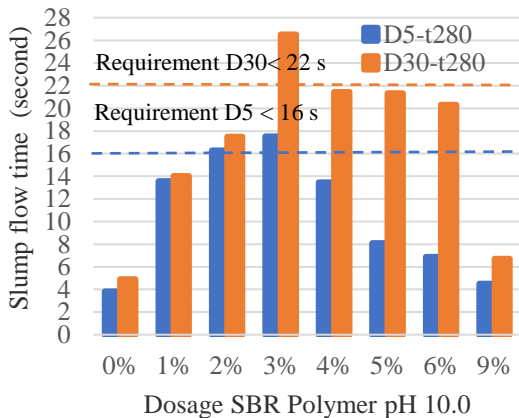
The polymer component contributes to the demulsification of asphalt emulsion, which can significantly decrease the workability of CAM [19]. The decreasing workability of CAM can be attributed to the intensive demulsification process of asphalt emulsion and the enhanced bonding between the asphalt coalescence and the cement hydration [29]. Demulsification of asphalt emulsion increases CAM

viscosity [31]. During this process, the asphalt coalescence bonds to cement hydration rapidly, resulting in a sharp increase in CAM viscosity [32]. It indicates an increase in the yield stress and viscoelasticity of fresh CAM. Consequently, this leads to a deceleration in funnel fluidity time and slump flow time. Higher yield stress in fresh CAM indicates decreased self-flowing ability [29].

The SBR polymer dosage of 4% to 6% in CAM led to an acceleration of funnel fluidity time from 118.3 s to 93.54 s, and their slump flow time D5-280 accelerated from 13.46 s to 6.89 s and D30-t280 from 21.46 s to 20.33 s. It is suspected that polymers contributed to increasing the stability of the mixture by delaying the asphalt emulsion demulsification process. This results in accelerated funnel fluidity time and slump flow time. The fresh CAM mixture shows a flow that is the same at different locations along the same flow path, indicating uniformity of slump flow, as shown in Fig. 12. e, f, g. In this condition, no agglomeration phenomenon occurs, which indicates a delay in the demulsification of asphalt emulsion [19].



a) Funnel fluidity time.



b) Slump flow time

Fig. 11 The effect of SBR polymer pH 10.0 dosage on funnel fluidity time and slump flow time of CAM

The improvement is attributed to the increased stability of the mixture, which delayed the demulsification process of asphalt emulsion [29]. The delayed process contributed to an acceleration funnel fluidity time and slump flow time. Polymer components in the mixture enhance its stability and delay the demulsification process, resulting in decreased viscosity and flowability. Adding polymer promoted ease of flow with minimal signs of agglomeration phenomena [19].

The SBR polymer dosage of 9% in CAM led to an acceleration slump flow time of 6.89 s for D5-t280 and 6.71 s for D30-t280, as shown in Fig. 11. b. However, this resulted in the non-uniformity of slump flow CAM, as presented in Fig. 12.h.

SBR polymer dosage of 1% to 6% in CAM results in compatibility between asphalt emulsion and cement. This case results in the low separation of hardened CAM < 3.0%, as shown in Fig. 13. However, a dose of 9% results in a separation rate of 10.88% > 3.0%. These results indicate a saturation point for the SBR polymer dosage in decreasing the separation rate of hardened CAM.

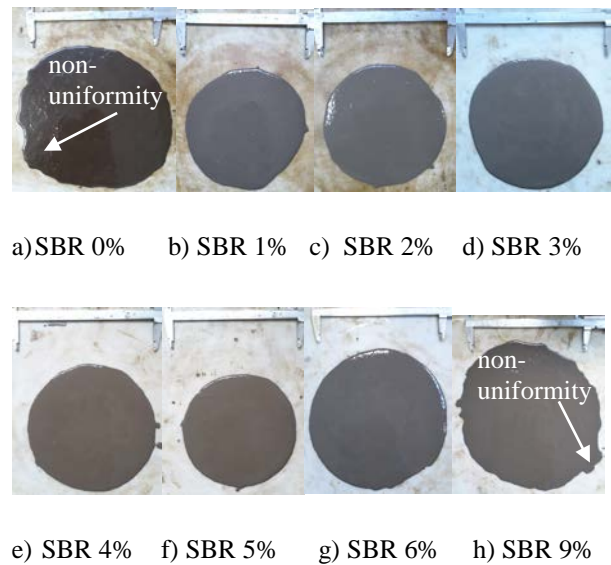


Fig. 12 The Effect of SBR polymer dosage on the uniformity flow of CAM

Liu B [15] reported that SBR polymer dosage of 1% to 4% resulted in much better properties of CAM. Zhang Y and Peng H reported that a polymer dosage of 6% resulted in significantly better interfacial bonding strength of CAM [7,14]. Zhang Y reported that 3% to 6% polymer improved the anti-corrosion ability of CAM [33]. Based on the recent results, SBR polymer pH 10.0 with a dosage of 4% to 6% resulted in the compatibility and workability of CAM.

## 5. CONCLUSIONS

Based on the result of the study, it can be concluded that increasing the pH value of the SBR polymer decreases the zeta potential of PMAE. Decreasing zeta



potential to neutral resulted in destabilizing asphalt droplets, demulsification, flocculation, separated water, and asphalt coalescence. During the hardening phase of the CAM structure, the asphalt coalescence layer covered by SBR polymer forms a binding film on cement, affecting the compatibility between PMAE and cement hydration. Compatibility between PMAE and cement is achieved by pH 10.0 SBR polymer doses ranging from 1% to 6%. The dosage of SBR polymer pH 10.0 of 1% to 3% in CAM led to a deceleration of slump flow time and funnel fluidity time. The dosage of SBR polymer pH 10.0 of 4% to 6% in CAM led to an acceleration of funnel fluidity time and slump flow time. The best compatibility and workability of CAM are proposed using the SBR polymer pH 10.0 dosage of 4% to 6%.

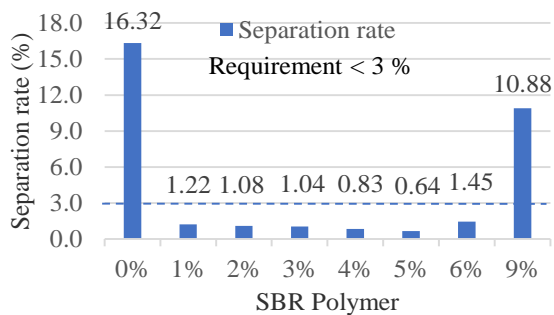


Fig.13 Effect of SBR polymer dosage on the separation rate of CAM.

## 6. ACKNOWLEDGEMENTS

The financial support from the Indonesia Endowment Fund for Education (LPDP) (0001559/TRP/D/ASN-AF-2019) (2020022130234) is gratefully acknowledged.

## 7. REFERENCE

- [1] Mayang S., and Muthohar I., Analysis on Railway Infrastructure Utilization Priority Factor Variation on Track Access Charges, *J. Civ. Eng. Forum*, vol. 2, no. 2, 2017, p. 197, doi: 10.22146/jcef.26584.
- [2] Pamungkas T.Y.D., and Muthohar I., The Issues of Track Maintenance Management in Indonesia (Based on Study of the British Railways), *J. Civ. Eng. Forum*, vol. 3, no. 1, 2017, p. 321, doi: 10.22146/jcef.26573.
- [3] Purba A., The Challenge of Developing High-Speed Rail Projects: Recent Evidence From Developing Countries, *Int. J. Geomate*, vol. 18, no. 70, 2020, pp. 99–105, doi: 10.21660/2020.70.9393.
- [4] Köllö S.A., Puskás A., and Köllö G., Ballasted Track Versus Ballastless Track, *Key Eng. Mater.*, vol. 660, no. 8, 2015, pp. 219–224, doi: 10.4028/www.scientific.net/KEM.660.219.
- [5] Aggestam E., and Nielsen J.C.O., Simulation of Vertical Dynamic Vehicle–Track Interaction Using a Three-Dimensional Slab Track Model, *Eng. Struct.*, vol. 222, no. 5, 2020, p. 110972, doi: 10.1016/j.engstruct.2020.110972.
- [6] Mao J., Zhang J., Feng Q., and Cao H., Influence of Emulsified Cement Asphalt Mortar Seam on Dynamic Characteristics of Vehicle-China Railway Track System II Ballastless Track System, *J. Eng. Sci. Technol. Rev.*, vol. 10, no. 6, 2017, pp. 52–61, doi: 10.25103/jestr.106.08.
- [7] Zhang Y., Cai X., Gao L., and Wu K., Improvement on the Mechanical Properties of CA Mortar and Concrete Composite Specimens in High-Speed Railway by Modification of Interlayer Bonding, *Constr. Build. Mater.*, vol. 228, 2019, p. 116758, doi: 10.1016/j.conbuildmat.2019.116758.
- [8] Cai X., Zhang Y., Gao L., Wang J., and Peng H., Deterioration of Cement Asphalt Pastes with Polymer Latexes and Expansive Agent Under Sulfate Attack and Wetting Drying Cycles, *Eng. Fail. Anal.*, vol. 109, no. 10, 2020, p. 104252, doi: 10.1016/j.engfailanal.2019.104252.
- [9] Fang L., Zhou J., Yang Z., Yuan Q., and Que Y., Interaction between Cement and Asphalt Emulsion and Its Influences on Asphalt Emulsion Demulsification, Cement Hydration, and Rheology, *Constr. Build. Mater.*, vol. 329, no. 3, 2022, p. 127220, doi: 10.1016/j.conbuildmat.2022.127220.
- [10] Nanthavisit P., Jitsangiam P., and Pichayapan P., Influence of Cement and Asphalt Emulsion Ratios on Cement-Asphalt Emulsion Mortar, *Int. J. Geomate*, vol. 17, no. 64, 2019, pp. 77–84.
- [11] Wang F., and Liu Y., The Compatibility and Preparation of the Key Components for Cement and Asphalt Mortar in High-Speed Railway, in book *Reliability and Safety in Railway*, X. Perpinya, Ed., Wuhan: in Tech D.O.O., 2012, pp. 223–260. doi: 10.5772/35722.
- [12] Yao Y., and Sun H., Performance and Microanalysis of Cement Asphalt Mortar with Admixture of Coal Fly Ash, *J. Mater. Sci. Res.*, vol. 1, no. 2, 2012, pp. 193–206, doi: 10.5539/jmsr.v1n2p193.
- [13] Li Y., Chen J., Wang J., Shi X., and Chen L., Study on the Interface Damage of CRTS II Slab Track Under Temperature Load, *Structures*, vol. 26, 2020, pp. 224–236, doi: 10.1016/j.istruc.2020.04.014.
- [14] Peng H., Zhang Y., Wang J., Liu Y., and Gao L., Interfacial Bonding Strength between Cement Asphalt Mortar and Concrete in Slab Track, *J. Mater. Civ. Eng.*, vol. 31, no. 7, 2019, p. 04019107, doi: 10.1061/(asce)mt.1943-5533.0002741.
- [15] Liu B., and Liang D., Effect of Mass Ratio of Asphalt to Cement on the Properties of Cement Modified Asphalt Emulsion Mortar, *Constr. Build. Mater.*, vol. 134, 2017, pp. 39–43, doi: 10.1016/j.conbuildmat.2016.12.137.



- [16] Liang P., Liang M., Fan W., Zhang Y., Qian C., and Ren S., Improving Thermo Rheological Behavior and Compatibility of SBR Modified Asphalt by Addition of Polyphosphoric Acid (PPA), *Constr. Build. Mater.*, vol. 139, 2017, pp. 183–192, doi: 10.1016/j.conbuildmat.2017.02.065.
- [17] Sreeram A., Filonzi A., Komaragiri S., Lakshmi Roja K., Masad E., and Bhasin A., Assessing the Impact of Chemical Compatibility of Additives Used in Asphalt Binders: A Case Study Using Plastics, *Constr. Build. Mater.*, vol. 359, no. 6, 2022, p.129349, doi 10.1016/j.conbuildmat.2022.129349.
- [18] Emtiaz M., Imtiyaz M.N., Majumder M., Idris I.I., Mazumder R., and Rahaman M.M., A Comprehensive Literature Review on Polymer-Modified Asphalt Binder, *Civil Eng.*, vol. 4, no. 3, 2023, pp. 901–933, doi: 10.3390/civileng4030049.
- [19] Ho T., Le M., Park D., Seo J., and Phan T.M., Anti-chemical Resistance, and Mock-up Test the Performance of Cement Asphalt Mortar Modified with Polymer for Ballast Stabilizing, *Constr. Build. Mater.*, vol. 232, 2020, p. 117260, doi: 10.1016/j.conbuildmat.2019.117260.
- [20] Fazhou W., Yunpeng L., and Shuguang H., Effect of Early Cement Hydration on the Chemical Stability of Asphalt Emulsion, *Constr. Build. Mater.*, vol. 42, 2013, pp. 146–151, doi: 10.1016/j.conbuildmat.2013.01.009.
- [21] Cui D., and Pang J., The Effect of pH on the Properties of a Cationic Bitumen Emulsifier, *Tenside, Surfactants, Deterg.*, vol. 54, no. 5, 2017, pp. 386–392, doi: 10.3139/113.110520.
- [22] Kumar A., and Dixit C.K., Methods for Characterization of Nanoparticles, in book *Advances in Nanomedicine for the Delivery of Therapeutic Nucleic Acids*, 2017, pp. 44–58. doi: 10.1016/B978-0-08-100557-6.00003-1.
- [23] Yildirim Y., Polymer Modified Asphalt Binders, *Constr. Build. Mater.*, vol. 21, no. 1, 2007, pp. 66–72, doi: 10.1016/j.conbuildmat.2005.07.007.
- [24] Zheng X., Liu, J., Zeng Z., Li S., Ding R., Xue Z., Weng Z., Zhong Y., and Ren H., Rheological Behavior, Segregation, Microstructure, and Construction Quality of Cement Emulsified Asphalt Mortar with Associative Thickener, *J. Mater. Civ. Eng.*, vol. 27, no. 11, 2015, pp. 2–9, doi: 10.1061/(asce)mt.1943-5533.0001278.
- [25] Lu C.T., Kuo M.F., and Shen D.H., Composition and Reaction Mechanism of Cement-asphalt Mastic, *Constr. Build. Mater.*, vol. 23, no. 7, 2009, pp. 2580–2585, doi: 10.1016/j.conbuildmat.2009.02.014.
- [26] Clogston J.D., and Patri A.K., Zeta Potential Measurement, in book *Methods in Molecular Biology*, vol. 697, 2011, pp. 63–70. doi: 10.1007/978-1-60327-198-1\_6.
- [27] Xiao J.J., and Jiang W., Study the Influence of Soap Solution's pH Value on the Modified Asphalt Emulsion Performance, *Appl. Mech. Mater.*, vol. 253–255, no. Part 1, 2013, pp. 312–316, doi 10.4028/www.scientific.net/AMM.253-255.312.
- [28] Plank J., and Gretz M., Study on the Interaction Between Anionic and Cationic Latex Particles and Portland Cement, *Colloids Surfaces a Physicochem. Eng. Asp.*, vol. 330, no. 2–3, 2008, pp. 227–233, doi: 10.1016/j.colsurfa.2008.08.005.
- [29] Ouyang J., Corr D.J., and Shah S.P., Factors Influencing the Rheology of Fresh Cement Asphalt Emulsion Paste, *J. Mater. Civ. Eng.*, vol. 28, no. 11, 2016, p. 04016140, doi: 10.1061/(asce)mt.1943-5533.0001653.
- [30] Islam G.M.S., Akter S., and Reza T.B., Sustainable High-performance, Self-compacting Concrete Using Ladle Slag, *Clean. Eng. Technol.*, vol. 7, no. 2, 2022, p. 100439, doi: 10.1016/j.clet.2022.100439.
- [31] Qiang W., Peiyu Y.A.N., Xiangming K., and Jinbo Y., Compressive Strength Development and Microstructure of Cement-asphalt Mortar, *J. Mater. Civ. Eng.* 23(9)1353-1359, vol. 26, no. 5, 2011, pp. 998–1003, doi: 10.1007/s11595-011-0351-9.
- [32] Ouyang J., Tan Y., Li Y., and Zhao J., Demulsification Process of Asphalt Emulsion in Fresh Cement-asphalt Emulsion Paste, *Mater. Struct. Constr.*, vol. 48, no. 12, 2015, pp. 3875–3883, doi: 10.1617/s11527-014-0446-9.
- [33] Zhang Y., Peng H., Gao L., Wang J., and Cai X., Effects of Polymer Latex and Expansive Agent on the Resistance of Cement Asphalt Pastes to Sulfuric Acid Attacks, *J. Mater. Civ. Eng.*, vol. 32, no. 6, 2020, p. 04020128, doi: 10.1061/(asce)mt.1943-5533.0003224.